

FE Fracture Prediction on Edges of Punched Holes

Dr Janka Cafolla, David P. Norman

Tata Steel UK Limited

1 Introduction

Many industry sources identified fracture from holes and edges as a key knowledge gap for fracture prediction of AHSS and UHSS grades. Ford Aachen with MATFEM cooperation [1] has shown an importance of including fracture failure models into their finite element (FE) simulations especially when designing with UHSS such as Boron Steel.

Hole expansion coefficient (HEC) is one of the ways to characterise the edge cracking of metals. Many studies investigated the best way of predicting the fracture using HEC in their experimental work [2], [3] combined with FE simulation [4]. In the later one a simplification for an FE simulation is done such that only 2D model is utilized. Since the study examines the area around the hole in quite a detail, the mesh density is too high for general use in crash FE model of a full vehicle.

In forming simulations HEC and forming limit curve (FLC) are often the criteria for inspecting the possibility of material failure. In crash simulations neither HEC nor FLC are generally used. More suited are the phenomenological fracture models which are more applicable for a wider range of engineering problems. There are now a number of these fracture models available. Examples of some of these fracture models are from Gurson [5] and various extensions to Gurson, Dell and Gese [6], Wierzbicki [7] and Wilkins [8].

Dell and Gese use CrachFEM material model developed by MATFEM [9]. Tata Steel adopted the use of CrachFEM material in past few years. Horn [10] and his colleagues at Tata Steel Research and Development have investigated several methods for measuring and analysing the data needed as input variables in CrachFEM material cards. CrachFEM material data are now available for the customers in AURORA material database. Norman and Buckley [11] have successfully used this data in their automotive virtual development process. Their test-FE correlation gave very promising results. CrachFEM material model has therefore become a winning tool for developing a simple method of fracture prediction in a crash event.

A simple rectangular test specimen with a hole in the middle was designed such that it was possible to use the optical strain measurement system - ARAMIS. This gave an opportunity to correlate not only force-displacement curves between the test and FE simulations but also strain development around the hole.

2 CrachFEM Material Model

CrachFEM is a phenomenological fracture model, originally developed by Dell and Gese from MATFEM for use with sheet materials in FE simulations of automotive structures, but is also available for use with thicker and/or non-ferrous materials. For thin sheet materials, CrachFEM combines two plasticity and failure models together. One model handles the necking behaviour of thin sheet due to tensile loading (Crach Sub-Model) and the other handles the dependency of fracture on the stress state (MF-GenYLD).

2.1 MF-GenYLD

The MF-GenYLD fracture model is an anisotropic material model that models fracture as a function of stress triaxiality. The model treats shear fracture (ductile shear fracture) and void growth (ductile normal fracture) as two distinct fracture modes, and describes a different fracture limit curve for each fracture mode [6]. In order to simplify the requirement for large numbers of material tests to describe the fracture limit curves, the fracture limit curves are described by mathematical functions to give a representative fracture curve shape. The ductile shear fracture function is based on the ratio of the maximum shear and von-Mises stresses. The ductile normal fracture function is based on a ratio of the hydrostatic and von-Mises stresses.

For the plasticity model in MF-GenYLD, a wide range of yield loci are available to choose from, allowing a wide range of materials to be modelled. A combined isotropic-kinematic hardening method is also used in order to represent the loading and unloading conditions caused by multi-step processes.

2.2 Crach Sub-Model

The Crach Sub-Model is a sub-routine within the CrachFEM fracture model, which is used to predict the onset of necking and instability in sheet materials due to tensile loading [12]. Essentially, it uses a forming limit curve (FLC) methodology that has been adapted to include non-linear strain paths and to allow the mapping of results from one simulation to another with different meshes. This enables multiple forming steps and the final crash simulation to be linked together, which is essential if the fracture behaviour of the sheet in its final condition is to be modelled.

2.3 Post-Critical Strain

The Crach Sub-Model also includes a Post-Critical-Strain (PCS) module for predicting fracture after the onset of necking instability [13]. The PCS method calculates a fracture strain from the plane strain, shear fracture limit and the element length, which gives some dependency of the fracture strain on the triaxiality of the stress state in the necking region.

3 Physical Test Set-up

Two AHSS materials were tested. Their basic material properties are listed in Tab. 1 as obtained from tensile tests of specimens without a hole to gain the stress-strain curves for FE simulations.

Tab. 1: Basic Mechanical Properties from tensile tests in rolling direction and clearance used for punched holes

	Thickness	Yield Strength	Tensile Strength	A _g	Clearance		
	[mm]	[MPa]	[MPa]	[%]	[%]	[%]	[%]
Material A	1.5	380	673	14.8	6.7	13.3	30.0
Material B	1.52	508	837	14.9	6.6	13.2	29.6

A simple rectangular test specimen with a hole in the middle (Fig. 1) was designed for this series of tests.

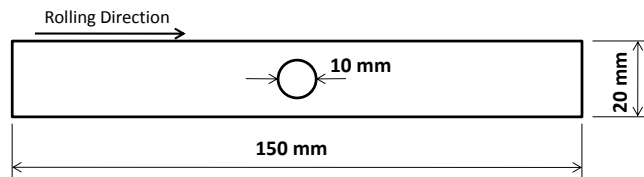


Fig. 1: Geometry of the test specimen

To create a variation in the quality of the edge of the hole, the samples were punched with different punch-die clearances (Fig. 2). Very good quality edges were punched with the Standard ISO/TS 16630 [14] recommended punch-die clearance of about 13% (Tab. 1) and the edges were polished. Very poor quality edges were created using either punch-die clearance of about 7% or 30% (Tab. 1) and a "blunt" punch has been applied. As shown in Fig. 2, the "blunt" punch has its corners rounded to make sure that the punch hole has rougher edges that it would have with a standard punch.

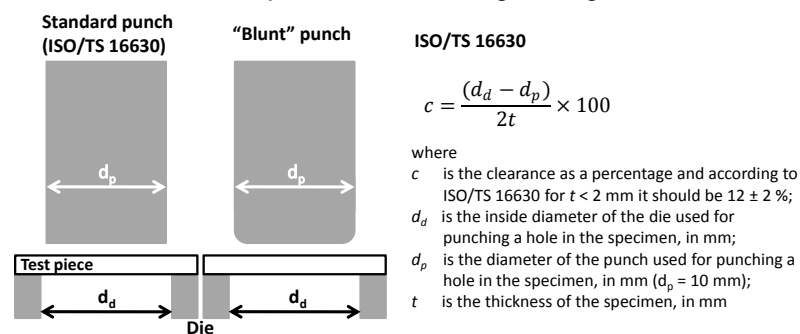


Fig. 2: Punch-Die set-up for creating different quality of edges

The tensile tests of the samples with a hole were done on MTS-300 kN tensile machine using also the optical strain measurement system - ARAMIS. The testing speed has been kept constant for all tests. The specimens were clamped such that the test length was 50 mm (50 mm clamped length on either side for a total specimen length of 150 mm).

Each specimen was transformed in 3D such that the Y-direction corresponded to the major strain direction. Therefore, there should ideally be only a minimal difference, if at all any, between the principal major strain and the directional Y-strain.

4 Virtual Test Set-up

The FE model of the test specimen has been created to reflect the real specimen as close as possible. The aim of this study is to find a way to weaken the edge elements around the hole such that the fracture initiation occurs earlier as it does for poor edge quality in real test. One of the methods to achieve this is to induce the artificial initial plastic strain on the elements surrounding the hole. Introducing the artificial initial strain does not mean that this is the strain condition of the material around the hole. The initial strain is simply a tool to force the elements at the edge to reach their critical elimination strain in advance and therefore fail earlier.

The method uses the *INITIAL_STRESS_SHELL_SET card in LS-DYNA® (see Fig. 3) which introduces the pre-strained elements around the hole at the start of the FE simulation. This weakens the edge elements and forces the element elimination earlier compared to the simulations without any pre-strain in it. Plastic strain value is given as the last 8th number on the through thickness layer's stress state. The stress state is not defined therefore left as 0.0. For CrachFEM, the plastic strain history variable has to be also defined.

```

$
$
$ =====
$ INITIAL cards
$ =====
$
$ *INITIAL_STRESS_SHELL_SET
$ 2
$ 1 5 1 0 0 0 0 0 5.0E-2
$ -0.66667 0.0 0.0 0.0 0.0 0.0 0.0 0.0 5.0E-2
$ 5.0E-2 0.0 0.0 0.0 0.0 0.0 0.0 0.0 5.0E-2
$ -0.33333 0.0 0.0 0.0 0.0 0.0 0.0 0.0 5.0E-2
$ 5.0E-2 0.0 0.0 0.0 0.0 0.0 0.0 0.0 5.0E-2
$ 0.0 0.0 0.0 0.0 0.0 0.0 0.0 0.0 5.0E-2
$ 5.0E-2 0.0 0.0 0.0 0.0 0.0 0.0 0.0 5.0E-2
$ 0.33333 0.0 0.0 0.0 0.0 0.0 0.0 0.0 5.0E-2
$ 5.0E-2 0.0 0.0 0.0 0.0 0.0 0.0 0.0 5.0E-2
$ 0.66667 0.0 0.0 0.0 0.0 0.0 0.0 0.0 5.0E-2
$ 5.0E-2
$
$

```

Fig. 3: DYNA keyword file card for initial strain input

The ring of elements surrounding the hole was pre-strained into 5%, 10%, 15%, 20%, 25% and 30% for Material A and additional simulation of 40% was done for Material B.

The stress-strain curves needed for the CrachFEM material cards were obtained from the standard tensile tests (no holes) of each grade. The rest of the CrachFEM material data came from the AURORA database.

5 Results and Discussion

Three sets of results were investigated: force-displacement curves, section strains and contour plots of the Major strain around the hole.

5.1 Force-Displacement Curves

In the physical test the displacement can be measured using the extensometer but these are limited to minimum length. ARAMIS, an optical strain measurement system, offers an opportunity to measure the “virtual” displacement over any length of the specimen which was captured by the camera. Fig. 4 shows a part of a test sample captured by the camera during the experiment and a part of an FE model.

During the test the camera captures the movements of points on the surface of the specimen created by a special spray. For a given resolution, ARAMIS system is then able to calculate the position of each point for each stage of the experiment thus the strain could be calculated too. Effectively the distance of two points at the opposite edges of the measured area could be calculated for each stage from the mesh similar to FE mesh. This is the “virtual” gauge length.

Two nodes are then found in the FE model, which are placed approximately in the same distance from the hole as in the two points chosen on the test specimen as shown in Fig. 4.

The resulting force-displacement curves for each test and simulation are shown in Fig. 5.

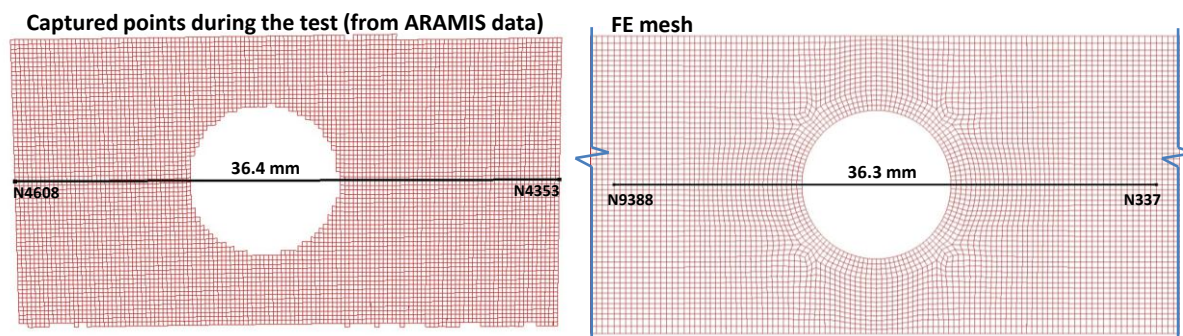


Fig. 4: Virtual gauge length in test and FE simulation

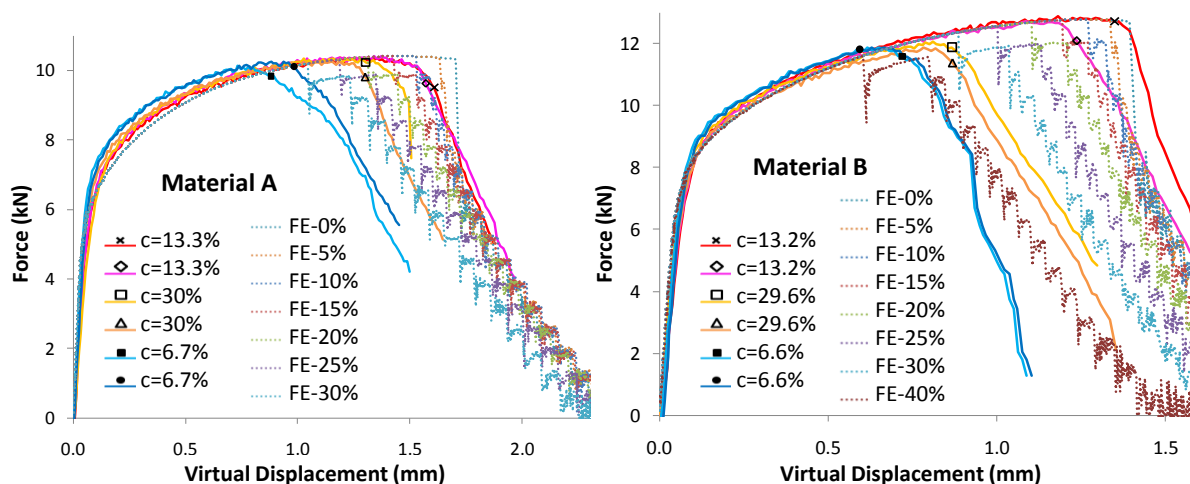


Fig. 5: Force-Displacement curves

Solid lines in Fig. 5 represent the tests and the dotted lines represent the FE simulations. The black markers on the individual curves from tests represent the point in time when the fracture on the test specimen was first observed. In FE simulation the fracture initiation is represented by the first vertical drop of the force-displacement curve when the first element reaches the critical elimination strain and is deleted.

From the tests it is clear that there is an influence of the poor edge on fracture of the material. For both materials the specimens with very good edges (polished edges created with punch-die clearance of about 13%) fractured later than the specimens with poor edges (edges created with punch-die clearance of about 7% or 30% and a blunt punch). Both material grades show slightly better performance of the samples created with punch-die clearance of about 30% compared to the specimens created with punch-die clearance of about 7%.

In FE simulation introducing the initial strains at the edge of the hole will cause the elements reach their critical elimination strain in advance and therefore fail earlier. Higher the initial strain, earlier the failure. This is clearly visible from the force-displacement curves.

Overlaying the FE simulations curves with test curves (Fig. 5) shows that the samples with very good edge quality represented by test samples created with punch-die clearance of about 13% fail approximately at the time as the FE models with about 5% to 10% pre-strain in the edge elements. The specimens created with the clearance of about 30% correspond to the FE models with about 20% pre-strain for Material A and 30% pre-strain for Material B. Punch-die clearance of about 7% created the specimens which for Material A correspond to the FE model with about 30% pre-strain. For Material B up to about 40% pre-strain is required in the edge elements of the FE model to match the test data.

5.2 Section Strains

As the sample is pulled, the major strains are rapidly increasing at both sides of the hole until the material fractures. The black markers on the test force-displacement curves in Fig. 5 indicate the fracture initiation in the tests. At this time the major strains were taken at each point across the entire width of the sample perpendicular to its longer edge and running through the two Stage points as shown in Fig. 6. The most left-hand side point of this section is assigned (0, 0) coordinates. The

distance of the rest of the points on the section from this point is then calculated from the measured coordinates on the undeformed shape.

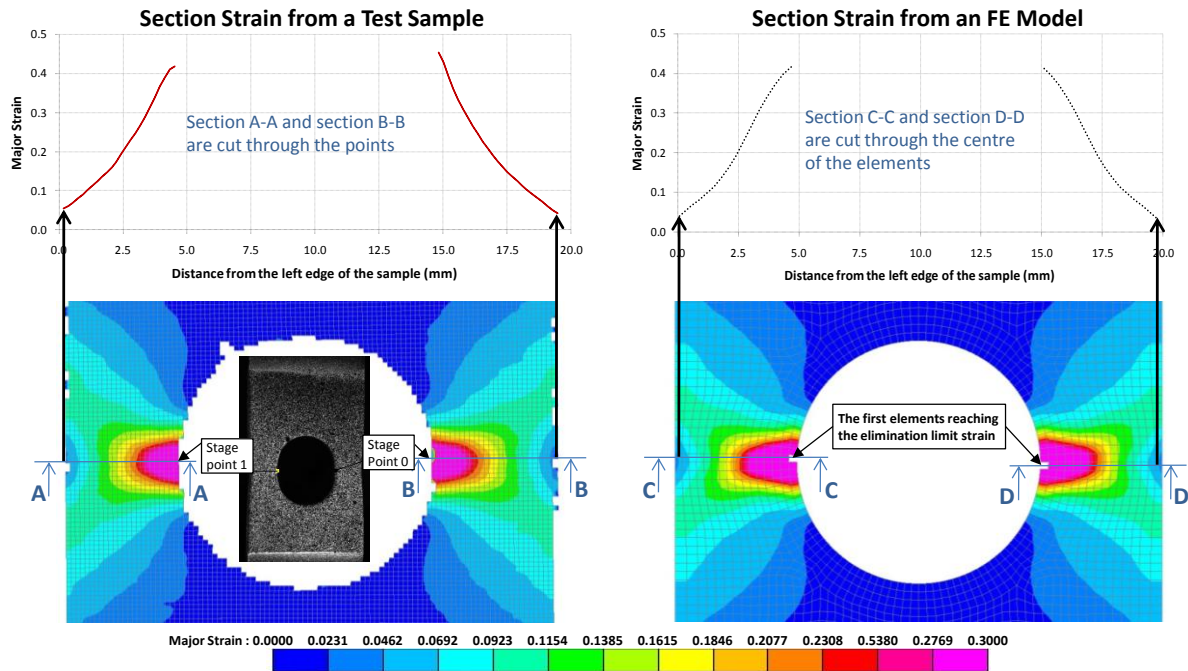


Fig. 6: Major Section strain obtained from test sample and FE model

In the FE simulations the major strains are element properties and they are calculated as a value per element and per element's through thickness integration point. Therefore a section through the sample's width would go through the middle of an element row. The top surface major strains are considered since the test measures the strains based on the sample's surface. The fracture initiation is represented by element elimination. When an element reaches the elimination limit strain, it is deleted from the model. The section major strain values are taken at the time just before the first element disappears. The distances from the left edge of the sample are calculated as coordinates of mid-points of each element in the row of elements where the section is cut on the undeformed shape.

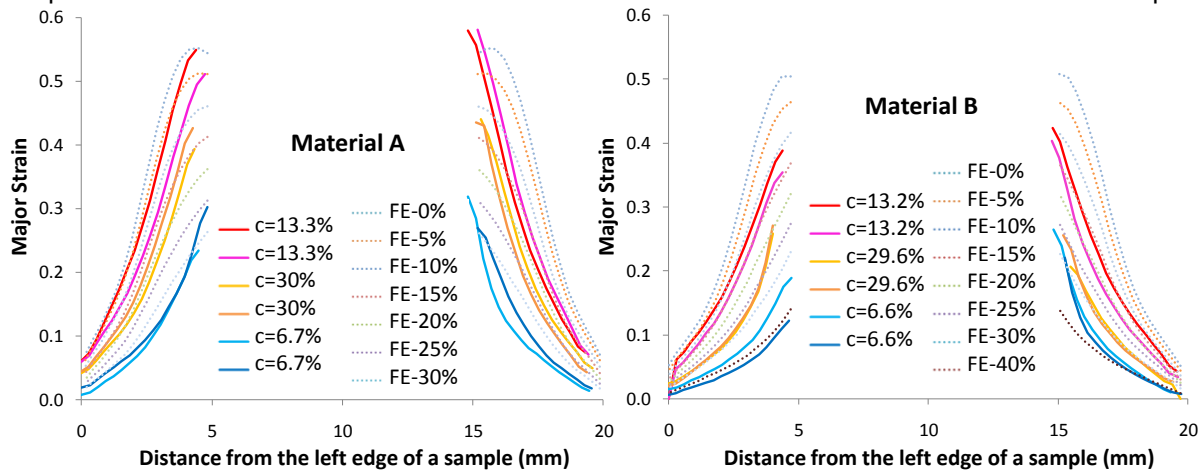


Fig. 7: Section Major Strain

Similarly as for the force-displacement curves the solid lines in Fig. 7 represent the tests and the dotted lines represent the FE simulations.

The general trend for the tests shows that at the time of failure the section major strain is higher for the good quality edge created with 13% clearance and polished than for the poor quality edges created with 7% or 30% clearance and blunt punch. The difference is very obvious.

The major section strain from FE simulations shows that as the initial strain in the elements around the hole is increased the section major strain at the time of failure decreases.

Overlaying the test curves with FE simulation curves (Fig. 7) shows a good match between test and FE. The results suggests that to represent the good quality punched edges a pre-strain of about 10% to 15% should be used on the elements surrounding the hole. If there is a concern about the punched

edge quality the pre-strain of up to 30% (maybe even 40% for higher strength grades) could be used to ensure the failure occurring earlier as it would with very rough edges.

5.3 Major Strain around the Hole

The ARAMIS system enabled to monitor the strain development around the hole for every stage during the test. This means that a contour plot of the major strain at the time when a fracture appears can be plotted. Fracture initiation in the test is indicated by markers in force-displacement curves (Fig. 5). This can be then compared to a contour plot of the major strain from FE simulation at the time just before the first element reaches the elimination strain and is deleted. Fig. 8 to Fig. 13 show this comparison. The contour plot scale has been set to same levels in both, tests and FE simulation. Both sets of results were post-processed in OASYS-D3PLOT software. In each figure the test results are on the left-hand side and FE simulation results are on the right-hand side. FE simulations results were chosen as closest match of the contour plot to the contour plot obtained from test results. Since only multiples of five were used as initial strain input, in some cases two or even three FE results are shown.

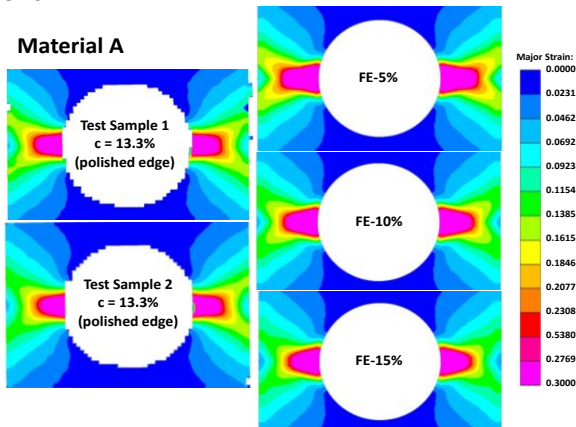


Fig. 8: Contour Plots of Major Strain for Material A and clearance 13.3%

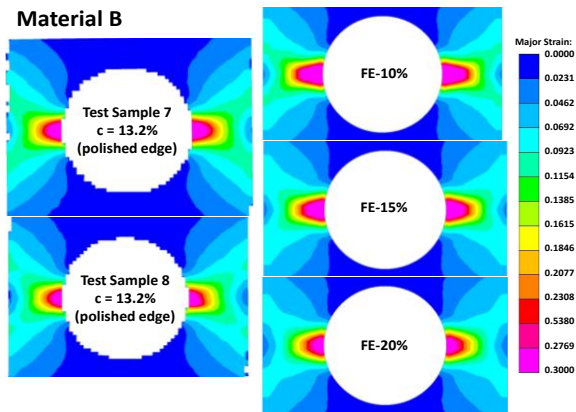


Fig. 11: Contour Plots of Major Strain for Material B and clearance 13.2%

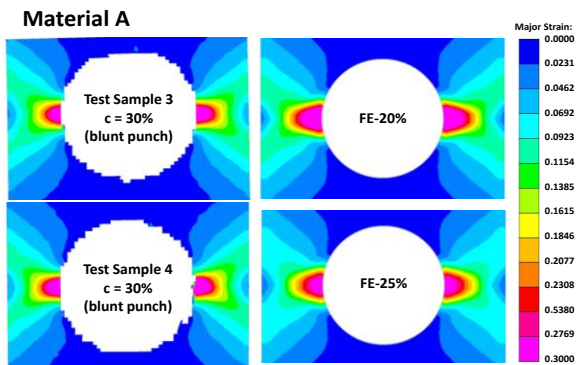


Fig. 9: Contour Plots of Major Strain for Material A and clearance 30%

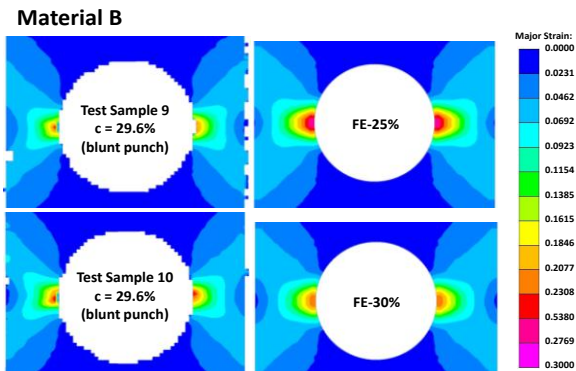


Fig. 12: Contour Plots of Major Strain for Material B and clearance 29.6%

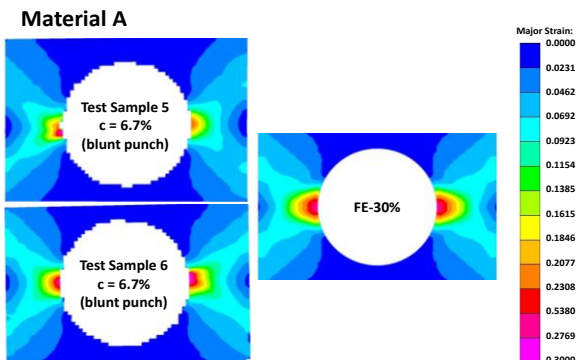


Fig. 10: Contour Plots of Major Strain for Material A and clearance 6.7%

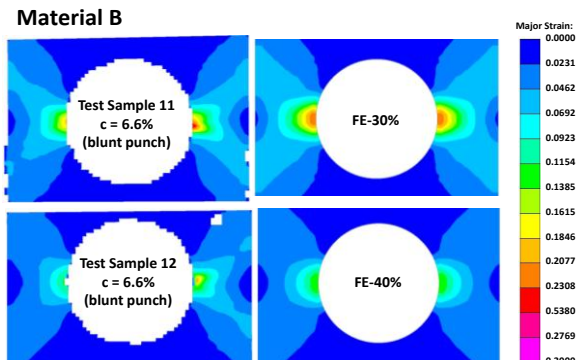


Fig. 13: Contour Plots of Major Strain for Material B and clearance 6.6%

Fig. 8 compares the Material A samples with polished edges and holes punched with punch-die clearance of 13.3% to the FE simulations. Three FE models with initial strain of 5%, 10% and 15% induced on the edge elements are shown here. The red area of the model FE-15% is the closest to the test samples' red areas. However, the rest of the contours – especially the yellow-green colours are better matched between the models FE-5% and FE-10% with the test samples. Overall, the model FE-10% is probably the closest match to both test samples 1 and 2.

Fig. 9 compares the Material A samples with holes punched with punch-die clearance of 30.0% and blunt punch to the FE simulations. Two FE models are shown here as the closest match to the test samples. FE-20% has yellow-green contours better matched to the test samples, while FE-25% has pink-red area closer tied with the test samples.

Fig. 10 compares the Material A samples with holes punched with punch-die clearance of 6.7% and blunt punch to the FE simulations. It is very clear here that the FE model with 30% pre-strain at the edge elements is the closest to the test samples results – especially to the test sample 6.

Fig. 11 compares the Material B samples with polished edges and holes punched with punch-die clearance of 13.2% to the FE simulations. As the test samples show the fracture appears at lower major strains compared to Material A. Therefore the corresponding FE models are the ones with higher initial strain induced to the edge elements. Yellow-green contours of FE-10% corresponds the best to the test sample 7 even though the pink-red contour of FE-15% (or even FE-20%) is probably the better match. Test sample 8 corresponds better to FE-15% or FE-20%.

Fig. 12 and Fig. 13 compare the Material B samples with holes punched with punch-die clearances of 29.6% and 6.6%, respectively, and blunt punch to the FE simulations. Test samples 9 and 10 (29.6% clearance) have their contour plots approximately like the FE model with 30% pre-strain in the edge elements. Test samples 11 and 12 (6.6% clearance) have their contour plots matched to somewhere between the FE models with 30% to 40% pre-strain in the edge elements – sample 12 is closer to 40% pre-strain model.

6 Summary

The aim of this study was to determine a simple way of representing rough edges in FE simulations. Introducing the initial strain into the elements along the edges has proven to be very simple and effective. The method considers the artificially created initial conditions in FE to weaken the edge elements aiming to initiate fracture earlier as it would at poor quality edge. This initial strain does not represent the actual strain state of the material.

Tab. 2: Summary of the results

	Approximate Clearance [%]		
	6-7	12-13 (ISO/TS 16630)	25-30
FE initial strain in edge elements for Material A [%]	30	10-15	20-25
FE initial strain in edge elements for Material B [%]	40	15	30

As Tab. 2 summarises, the correlation between the test and FE shows that if the artificial initial strain of about 10% to 15% is introduced into the elements around a hole in FE simulation, the predictions of fracture initiation correlates well with punch-die clearance of about $12 \pm 2\%$. This is the recommended punch-die clearance for the given thickness as per standard to create a reasonably good quality edges. Poor quality edge is often a results of using very small ($\approx 7\%$) or very large ($\approx 30\%$) punch-die clearance. To represent such poor edges in FE, a pre-strain of up to 30% in the elements around a hole can be used.

The study also suggests that the higher strength material would need to consider slightly higher initial strain conditions to account for poor quality edge.

The validation of this study recommendation should follow by looking at the more complex component with more complex loading conditions which is a part of the follow up investigation to be undertaken in Tata Steel R&D department.

7 Acknowledgement

The authors would like to express their gratitude towards Dr. Tushar Khandeparkar and his colleagues who had performed the physical tests at the laboratories of Joining and Performance Technology Group in IJMuiden, The Netherlands.

8 References

- [1] Lanzerath, H.; Bach, A.: "Potential of Boron Steels and Failure Modelling for Crash", International Automotive Body Congress, Vaals, The Netherlands, June 10-11, 2008
 - [2] Hyun, D.I., Oak, S.M., Kang, S.S., Moon Y.H.: "Estimation of Hole Flangeability for High Strength Steel Plates", ELSEVIER Journal of Materials processing Technology 130-131 (2002)
 - [3] Watanabe, K., Tachibana, M., Koyanagi, K., Motomura, K.: "Simple Prediction Method for the Edge Fracture of Steel Sheet During Vehicle Collision", LS-DYNA Anwenderforum, Ulm 2006
 - [4] Sartkulvanich, P., Kroenauer, B., Golle, R., Konieczny, A., Altan T.: "Finite Element Analysis of Effect of Blanked Edge Quality upon Stretch Flanging of AHSS", ELSEVIER CIRP Annals – Manufacturing Technology 59 (2010)
 - [5] Gurson, L., Eng J.: "Continuum Theory of Ductile Rupture by Void Nucleation and Growth: Part I - Yield Criteria and Flow Rules for Porous Ductile Media", Material Technology. Volume 99, Issue 1, 2 (1977)
 - [6] Hooputra, H., Gese, H., Dell H., Werner, H.: "A comprehensive failure model for crashworthiness simulation of aluminium extrusions", International Journal of Crashworthiness, Volume 9, Issue 5 (2004)
 - [7] Wierzbicki, T., Bao, Y., Lee, Y-W., Bai, Y.: "Calibration and evaluation of seven fracture models", International Journal of Mechanical Sciences, Vol. 47, Nr. 4-5 , p. 719 – 743 (2005)
 - [8] Wilkins, M.L., Streit, R.D., Reaugh, J.E.: "Cumulative-strain-damage model of ductile fracture: simulation and prediction of engineering fracture tests", Tech. rep. UCRL-53058, Lawrence Livermore Laboratory, University of California, Livermore, CA 94550 (1983)
 - [9] "MF GenYld + CrachFEM Theory and LS-DYNA User's Manuals", Version 4.0; MATFEM; August 2007
 - [10] Horn, C. ten: „Testing Methods for Fracture Modelling of Sheet Steel“, Tata Steel; MATFEM conference; October 2012
 - [11] Buckley, M. A., Norman, D. P.: "Validation of a Virtual Method for Fracture Prediction in the Automotive Body Structure: a Key Enabler for Light Weight Vehicles", C1321 – Innovations in Fuel Economy and Sustainable Road Transport; IMechE Conference; Pune; India; November 2011
 - [12] Dell, H., Gese, H., Keßler, L., Werner, H., Hooputra, H.: "Continuous failure Prediction Model for Nonlinear Load Paths in Successive Stamping and Crash Processes", SAE Technical Paper Series 2001-01-1131
 - [13] Kessler, L., Gese, H., Metzmacher, G., Werner, H.: "An approach to model sheet failure after onset of localized necking in industrial high-strength steel stamping and crash simulations", SAE World Congress. April 14-17, 2008, Cobo Center, Detroit, Michigan, USA
 - [14] Technical Specification: "Metallic Materials – Method of Hole Expanding test", ISO/TS 16630, 2003
-